MULTI-SCALE ANALYSIS OF THERMO-MECHANICAL PROPERTIES OF 2.5D ANGLE-INTERLOCK WOVEN SHAPE MEMORY POLYMER COMPOSITES

H. Y. Sun

State Key Laboratory of Mechanics and Control of Mechanical Structures
Nanjing University of Aeronautics and Astronautics
Nanjing, China

J. P. Gu*

Jiangsu Key Laboratory of Advanced Structural Materials and Application Technology
Nanjing Institute of Technology
Nanjing, China

State Key Laboratory of Mechanics and Control of Mechanical Structures
Nanjing University of Aeronautics and Astronautics
Nanjing, China

Y. Tang

State Key Laboratory of Mechanics and Control of Mechanical Structures
Nanjing University of Aeronautics and Astronautics
Nanjing, China

Z. M. Xie*

Center for Composite Materials and Structures
Harbin Institute of Technology
Harbin, China

ABSTRACT

A multi-scale strategy is employed in the paper to investigate the thermo-mechanical properties of 2.5D angle-interlock woven shape memory polymer composites (SMPCs). In the study, the mesoscopic model of 2.5D woven SMPCs and microscopic model of yarns are firstly developed. After that, the themo-viscoelastic constitutive relationship of the yarn is described in the form of hereditary integral and the parameters of relaxation moduli are obtained from nonlinear fitting of Prony series based on the results of finite element method (FEM). Based on the multi-scale models and the constitutive relationship, the effects of warp and weft arranged densities on viscoelastic properties of 2.5D woven SMPCs are studied in detail. Finally, the shape memory behavior along the warp direction in small strain region is also analyzed. The research in the paper lays a foundation for design and application of woven SMPCs in engineering.

Keywords: Multi-scale analysis, Woven shape memory polymer composites, Thermo-mechanical property, Shape memory behaviors.

1. INTRODUCTION

Shape memory polymers (SMPs) have received much attention worldwide since 1980s due to their advantages, such as excellent shape recoverability, low density, easy controllability in shape memory behaviors, especially low cost [1]. However, the recovery force of SMPs is small as compared with that of shape memory alloys, and the recovery speed is low. Shape memory polymer composites (SMPCs) are developed to achieve high recovery force and recovery speed [2]. Besides, some of them also have the ability to enhance or enable new

* Corresponding author (gujianping@njit.edu.cn; xiezhm@hit.edu.cn)

DOI : 10.107/jmech.2018.48
Copyright © 2018 The Society of Theoretical and Applied Mechanics
https://doi.org/10.1017/jmech.2018.48 Published online by Cambridge University Press

stimulus approaches and novel SMEs. The potential application of SMPs and SMPCs is rather broad, ranging from clothing manufacturing, temperature sensors, intelligent biomedical devices to self-deployable structures in aeronautics and astronautics [3-5].

Generally, the particulate-filled and straight fiber reinforced SMPCs are the two main categories of SMPCs. The former cannot be applied in large-scale structures due to the poor integrated mechanical properties while the latter may reduce the shape deformability along the fiber direction. With the rapid development of textile technology, woven fabric reinforced SMPCs (woven SMPCs for short) with superior delamination resistance and fairly good shape deformability have become the cutting edge in the field. Recently, morphing technology on aircraft has attracted many researchers in aeronautics. The essential condition for the morphing aircraft structures is that it can be able to change its shape and carry the required load. Since the aircraft structures are mainly stiff, the morphing wing requires the variable stiffness skin materials to guarantee the deformation of the structure while maintaining structural integrity and load-bearing capability. For the woven SMPCs can significantly change their stiffness upon heating or cooling, they may have great potential as the variable stiffness skin materials. Although the woven SMPCs may have broad application in aeronautics and astronautics, the mechanism for their thermo-mechanical behaviors and shape memory effects are still indefinite which also limits their practical application.

To date, some work has been conducted to study the thermo-mechanical behavior of woven SMPCs, mainly concentrated on shape recovery ratio and recovery stress. Zhang *et al.* [6] studied the bending recovery behavior of woven SMPCs. The deformation recovery ratios were compared with those of the pure SMP samples. They also proposed an analytical model to predict the bending recovery ratio of the SMP based laminates, in which the woven fabric reinforcement was simplified as an isotropic material. Ahmad *et al.* [7] investigated the deterioration of mechanical properties of a polystyrene-based woven SMPC under tensile loads. It was found that the material shows good shape recovery ability as the strain is less than 100%. Owing to the delamination and the failure of fibers, low recovery ratios were observed for samples under the strain larger than 100%. Roh *et al.* [8] studied the recovery rate of woven SMPCs and established a new numerical model based on experimental data. Recently, the healing ability of SMPCs for impact damage has attracted much attention. Woven SMPCs with impact tolerance and self-healing ability have been studied. Nji and Li [9] carried out a series of experiments on 3D woven SMPCs to investigate the failure modes and evaluate its self-healing capability. It was shown that healing efficiency is greatly dependent on the impact energy. It should be noted that though the impact tolerance and service life are improved by the 3D woven SMPCs, the materials still would be perforated at the macro-length scale after several impact. The reason is that various types of non-healable damage such as fiber/matrix interfacial debonding, fiber fracture, etc, occur at the micro-length scale. This should be the challenge for the fabrication of 3D woven SMPCs with self-healing capability.

The mesostructure of woven fabric reinforced composites, especially 3D woven composites, is rather complicated. The yarn bundles composed of the matrix and fibers intertwine in all three principle directions. In order to predict the thermo-mechanical properties of woven SMPCs as accurately as possible, a multi-scale method can be used. Hence, to establish a mechanical model which is reasonable and close to the real mesostructure of the composites is a prerequisite for the study. So far, a lot of numerical methods have been proposed to study the elastic performance of woven composites. Tan *et al.* [10, 11] put forward an analytical model based on iso-stress and iso-strain assumption to estimate the elastic constants and thermal expansion coefficients of 3D woven composites. Hallal *et al.* [12] presented an improved model, in which a three stages homogenization method was used to predict the elastic constants of 2.5D angle-interlock woven composites. A good agreement was shown between experimental data and analytical results. Recently, finite element modeling approach and the multi-scale analysis strategy have also been used to predict the mechanical properties with consideration of the complex structure of woven composites. Lu *et al.* [13] studied the progressive damage of 2.5D woven composites with multi-scale methods. In addition, the influence of off-axis angles on the failure behaviors of the matrix and yarns in woven composites was analyzed in the work. Song *et al.* [14, 15] proposed a new parameterized model named as Full-cell model in which both inner cells and surface cells were considered. Compared to Inner-cell model, Full-cell model with surface cells taken into account could get better predictions on elastic moduli along warp and weft directions. It can be seen that with the development of the research, the mesostructure model of the three-dimensional woven composites is getting closer to the real internal structure of the composites, so that the material properties can be more accurately predicted.

It is worth noting that the matrix of woven SMPCs is SMP which makes it different from common woven composites. The existing models for SMPs basically fall into two categories: the phase transition models and the thermoviscoelastic models. The phase transition models are firstly proposed by Liu *et al.* [16] and the thermo-viscoelastic models are firstly introduced by Tobushi *et al.* [17, 18] and further developed by Diani *et al.* [19] and Nguyen *et al.* [20]. Recently, Diani *et al.* [21] also revealed that the shape memory behavior of an epoxy network under small-strain deformation could be well predicted through a viscoelastic model combined with Time-Temperature Superposition Principle.

In this paper, the multi-scale method is adopted to study the thermo-viscoelastic properties of one kind of woven textile reinforced SMPCs, named as 2.5D angle-interlock woven fabric reinforced SMPCs (2.5D woven SMPCs for short). Firstly, the micro-scale representative unit cell (RUC) of the yarn and the meso-RUC of the woven composites are established, respectively. Thereafter, the viscoelastic parameters of the yarn are derived in our work. Furthermore, the programming method of user-defined material subroutine (UMAT) of ABAQUS

https://doi.org/10.1017/jmech.2018.48 Published online by Cambridge University Press

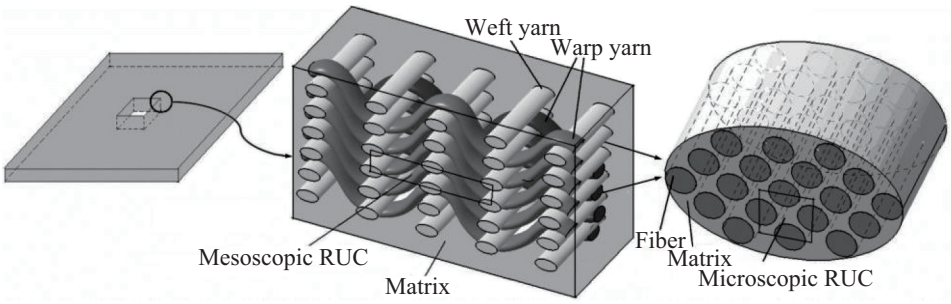


Fig. 1 The multi-scale models [22].

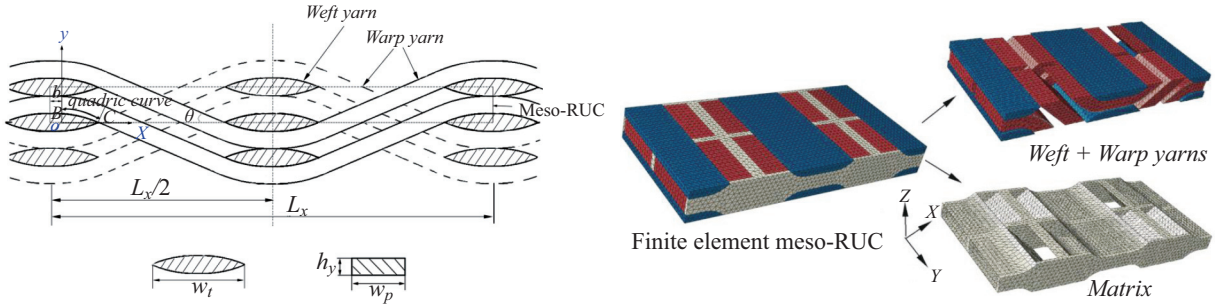


Fig. 2 (a) The geometric relation in the meso-RUC, and (b) the finite element meso-RUC of 2.5D woven SMPCs ($N_t = 6$, $N_p = 11$).

for the orthogonal viscoelastic materials is proposed here. Finally, the influence of weaving densities on viscoelasticity is investigated and the shape memory behavior of 2.5D woven SMPCs is also studied in the paper. The main difference between the paper and previous work is that the thermo-mechanical behaviors and the shape memory effects of the 2.5D woven SMPCs are studied for the first time by using the finite element approach from micro-scale and meso-scale respectively. Besides, the influencing factors are presented in the paper. Therefore, the research findings can be used to provide guidance for reasonable design of the 2.5D woven SMPCs in the potential applications.

2. MULTI-SCALE MODELS

In this section, the multi-scale modeling approach is applied to establish the mesoscopic model of 2.5D woven SMPCs and microscopic model of yarns, respectively. The modeling approach can be illustrated by Fig. 1.

2.1 Modeling of 2.5D Woven SMPCs

In the paper, the 2.5D angle-interlock woven composites with the weft yarns interlocked with two layers of warp yarns in the thickness direction will be studied. Since the inner part accounts for the most part of the woven composites, only the interior cell is studied in this paper. Therefore, the interior cell can be used as the meso-RUC of the 2.5D woven SMPCs as shown in Fig. 1. For simplicity, several assumptions are made as follows: (1) the cross section of warp yarns is regarded as rectangular shape; (2) weft yarns and warp yarns have the same cross-sectional area which keeps unchanged along their tracks; (3) weft yarns are straight while the tracks of warp yarns are assumed to be straight lines combined with quadric curves; (4) the heights of the cross-section of all the yarns are the same.

The idealized model of the meso-RUC is shown in Fig. 2(a). The longitudinal and transverse lengths, L_x and L_y, can be obtained from the woven parameters.

$$L_x = (10/N_t)\times 2, \quad L_y = (10/N_p)\times 2 \tag{1}$$

where N_t and N_p are the warp and weft arranged densities (tows/cm), respectively. The cross-sectional area of the yarn A can be calculated from the equation below

$$A = \frac{T}{1000\rho P}. \tag{2}$$

where T is the density of the yarn and ρ is the material density. P is the packing factor of fibers in the yarn, which can be calculated from the micro-RUC of yarns as presented in the next subsection. The weft and warp yarns are both composed of glass fibers. Some part of the outline of the weft yarn, from Point B to C, is assumed as a quadric curve which can be described as:

$$f = ax^2 + c \tag{3}$$

https://doi.org/10.1017/jmech.2018.48 Published online by Cambridge University Press

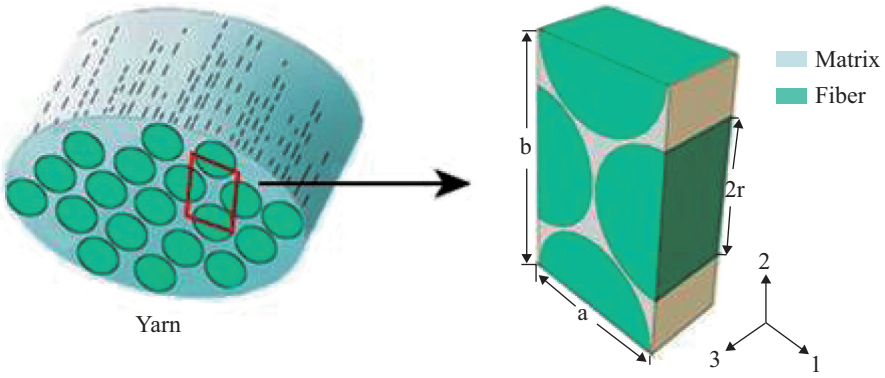


Fig. 3 Micro-RUC of the yarn.

Thus the length b of the straight section of weft yarns, coefficients of the quadric curve, width of the weft yarn w_t, width of the warp yarn w_p and dip angle θ can be obtained based on the assumptions above through the geometric relationships below.

$$-\tan\theta = 2a\left(\frac{w_t}{2}-b\right), \quad \tan\theta = \frac{L_z}{\frac{L_x}{2}-w_t-\frac{w_p}{\sin\theta}} \tag{4}$$

$$c=\frac{h_y}{2}, \quad a\left(\frac{w_t}{2}-b\right)^2+c=0 \tag{5}$$

$$4\left(\int_0^{w_t/2-b}(ax^2+c)dx+b\frac{h_y}{2}\right)=A \tag{6}$$

where L_z and h_y are the heights of the RUC and the yarn respectively, as illustrated in Fig. 2(a). Here, the finite element meso-RUC of 2.5D woven SMPCs is shown in Fig. 2(b).

2.2 Modeling of Micro-RUC of Yarns

In order to study the thermo-viscoelastic properties of the meso-RUC of the woven composites, we firstly should develop the micro-RUC of the yarns. The glass fibers are used in the yarns. As one kind of SMP, an acrylate polymer network is used as the matrix and the themomechanical properties of the material were well studied by Arrieta and Diani [23]. In addition, the thermo-mechanical modeling approach was developed for the acrylate polymer network, and the shape memory effects of the SMP were well predicted in the work of Arrieta and Diani [23]. Yarns can be considered as unidirectional fiber reinforced composites. Considering the uniformity of fiber distribution, a transverse isotropic periodic model can be used as the micro-RUC for the yarns. In the work, a rectangular parallelepiped micro-RUC, on which periodic boundary conditions can be easily applied, is adopted here as illustrated in Fig. 3. Based on the micro-RUC of yarns, the packing factor P in Eq. (2) can be derived as follows:

$$P=\frac{2\pi r^2}{ab} \tag{7}$$

where r is the radius of the fiber and $b=\sqrt{3}a$.

3. CONSTITUTIVE MODEL AND PROGRAMMING METHOD FOR YARN

3.1 Thermo-Viscoelastic Constitutive Model for Yarn

The relaxation-type constitutive model for viscoelastic materials at a constant temperature can be described in the form of hereditary integral as follows:

$$\sigma_i(t)=\int_{0^-}^{t} C_{ij}(t-\tau)\frac{d\varepsilon_j(\tau)}{d\tau}d\tau, \quad (i,j=1,2,\cdots,6) \tag{8}$$

where $C_{ij}(t)$ is the relaxation modulus.

The viscoelastic behaviors of thermo-rheological materials follow the Time-Temperature Superposition Principle. The relationship between the relaxation modulus at temperature T and the relaxation modulus at reference temperature T_0 can be described as

$$C_{ij}(T,t)=C_{ij}(T_0,\xi) \tag{9}$$

where $\xi = t/a_T$ is defined as reduced time from T to T_0, and a_T is a function of temperature. If the temperature changes continuously with time, the reduced time should be expressed by the following integral form.

$$\xi=\int_{0^-}^{t} 1/a_T(T(\tau))d\tau \tag{10}$$

The Williams-Landel-Ferry (WLF) equation can be used to characterize the change of the shift factor a_T with temperature.

$$\log a_T=-\frac{C_1(T-T_0)}{C_2+T-T_0} \tag{11}$$

where C_1 and C_2 are positive constants depending on material properties.

Using the equations above, the viscoelastic constitutive relationship of the yarn can be written as

https://doi.org/10.1017/jmech.2018.48 Published online by Cambridge University Press

$$\sigma_i(t)=\int_{0^-}^{t} C_{ij}(T_0,\xi_1-\xi_2)\frac{\partial}{\partial\tau}(\varepsilon_j(\tau)-\alpha_j(T(\tau)-T_0))d\tau,$$
$$(i,j=1,2,3,\cdots,6) \tag{12}$$

where α_j is the thermal expansion coefficient, $\xi_1=\int_{0^-}^{t}1/a_T(T(\tau'))d\tau'$ and $\xi_2=\int_{0^-}^{\tau}1/a_T(T(\tau'))d\tau'$. Thus the UMAT for ABAQUS can be written with the material Jacobian matrix based on the constitutive model above. The programming method is elucidated in Section 3.

The relaxation modulus of the yarn can be expressed as

$$\left[C_{ij}(t)\right]=\begin{bmatrix} C_{11}(t) & C_{12}(t) & C_{13}(t) & 0 & 0 & 0\\ C_{12}(t) & C_{11}(t) & C_{13}(t) & 0 & 0 & 0\\ C_{13}(t) & C_{13}(t) & C_{33}(t) & 0 & 0 & 0\\ 0 & 0 & 0 & C_{44}(t) & 0 & 0\\ 0 & 0 & 0 & 0 & C_{44}(t) & 0\\ 0 & 0 & 0 & 0 & 0 & C_{66}(t) \end{bmatrix} \tag{13}$$

where all entities are relaxation functions of time. These functions can be derived by applying six simple loading cases on the micro-RUC model (*i.e.*, uniaxial tensile loadings in three primary directions respectively and three pure shear loadings) with applied periodic boundary conditions.

The isotropic glass fiber is used in the micro-RUC of the yarns, and the elastic modulus, Poisson's ratio and thermal expansion coefficient of the fiber are 72 GPa, 0.2 and 5×10^{-6}/°C, respectively. As mentioned above, it is proved that the thermo-mechanical behavior of the SMP matrix can be well modeled by the approach developed by Arrieta and Diani [23]. Specifically, it is considered that the shape memory effects of the SMP can be predicted by assuming that the thermo-mechanical property of the SMP solely depends on the material viscoelasticity coupled with its time-temperature superposition property. In the approach, the generalized Maxwell model and the WLF equation were used to describe the viscoelastic behavior obtained by dynamic mechanical analysis (DMA) experiment and the time-temperature superposition principle, respectively. Since both the generalized Maxwell model and the WLF equation are already programmed in ABAQUS, it only needs an easy and standard use of the code. It should be noted that the same modeling approach is also adopted in our work for the same SMP material used in Arrieta and Diani [23]. Therefore the parameters for the acrylate polymer network can be directly obtained from Arrieta and Diani [23].

In the condition of small deformation, the elastic response of the yarn is assumed to be linear. Thus, the Prony series can be written as

$$f(t)=a+\sum b_i e^{-t/\tau_i}\quad (i=1,2,3,4) \tag{14}$$

The fitting curves of the relaxation functions of the yarn at 80°C are shown in Fig. 4.

For a two phase unidirectional fiber reinforced composite, thermal expansion coefficients of the yarn can be obtained from the model established by Schapery [24] based on energy principles. Therefore, the thermal expansion coefficient in the longitudinal direction can be expressed as

$$\alpha_3=(E_f\alpha_f\varphi_f+E_m\alpha_m\varphi_m)/(E_f\varphi_f+E_m\varphi_m) \tag{15}$$

and the thermal expansion coefficient in the transverse direction can be written as

$$\alpha_1=\alpha_2=(1+\mu_f)\alpha_f\varphi_f+(1+\mu_m)\alpha_m\varphi_m -\alpha_3(\mu_f\varphi_f+\mu_m\varphi_m) \tag{16}$$

where α, E, μ and φ are the thermal expansion coefficient, elastic modulus, Poisson's ratio and volume fraction, respectively. The subscript m and f refer to the matrix and fiber.

To verify the validity of the modeling method and the constitutive relationship above, the FEM results of creep behaviors with constant force applied in directions 1 and 3 of the yarn are compared with experimental data reported by Megins and Varna [25]. Figure 5 shows a good agreement between the experimental data and FEM results, which validates the modeling of the yarn.

3.2 Programming Method of UMAT

Here, the programming method of UMAT in ABAQUS for orthotropic viscoelasitic materials is introduced as follows. The stresses of the element must be updated at the end of each increment in UMAT. Substituting Eq. (14) into Eq. (8) gives

$$\sigma_i(t)=\int_{0^-}^{t}(a_{ij}+b_{ijk}e^{-(\xi_1-\xi_2)})(\dot{\varepsilon}_j(\tau)-\alpha_j\dot{T}(\tau))d\tau =\sum_{j=1}^{3}\left(M_{ij}(t)+\sum_{k=1}^{\kappa}N_{ijk}(t)+J_{ij}(t)+\sum_{k=1}^{\kappa}K_{ijk}(t)\right) \tag{17}$$

where

$$M_{i1}=\int_{0^-}^{t}a_{i1}\dot{\varepsilon}_1(\tau)d\tau,\quad N_{i11}(t)=\int_{0^-}^{t}b_{i11}e^{-(\xi_1-\xi_2)}\dot{\varepsilon}_{1(\tau)}d\tau,$$
$$J_{i1}=-\int_{0^-}^{t}a_{i1}\alpha_1\dot{\varepsilon}_1(\tau)d\tau,\quad K_{i11}(t)=-\int_{0^-}^{t}b_{i11}\alpha_1e^{-(\xi_1-\xi_2)}\dot{T}_{(\tau)}d\tau$$

and κ equals the order of Prony series used to fit the relaxation functions.

Thus the change of stress after Δt can be expressed as

$$\Delta\sigma_i(t)=\sum_{j=1}^{3}\left(\Delta M_{ij}(t)+\sum_{k=1}^{\kappa}\Delta N_{ijk}(t)+\Delta J_{ij}(t)+\sum_{k=1}^{\kappa}\Delta K_{ijk}(t)\right) \tag{18}$$

For example, M_{i1} and N_{i11} at the end of the time increment can be written as

$$M_{i1}(t+\Delta t)=\int_{0^-}^{t+\Delta t}a_{i1}\dot{\varepsilon}_1d\tau \tag{19}$$

https://doi.org/10.1017/jmech.2018.48 Published online by Cambridge University Press

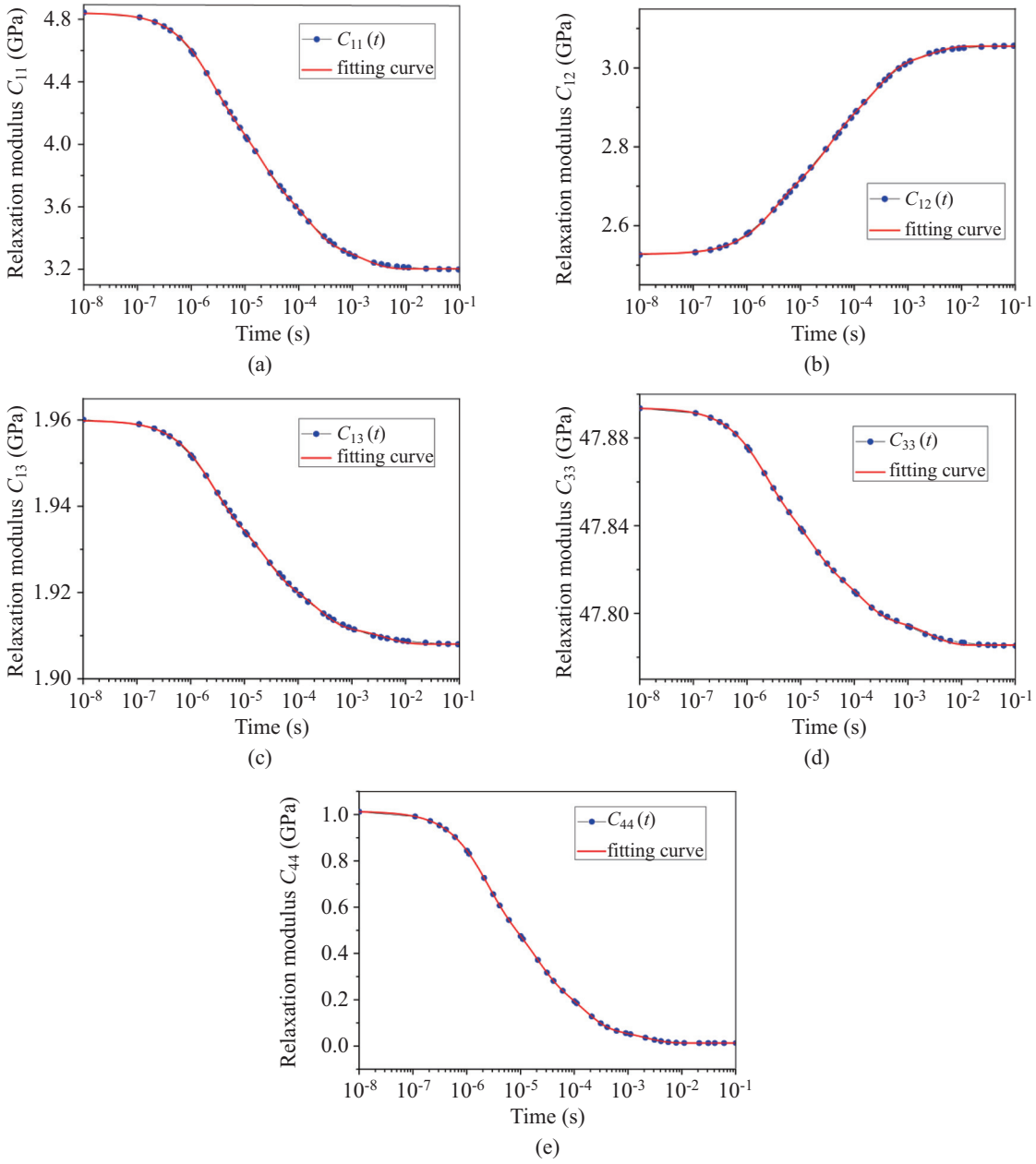


Fig. 4 Parameter fitting for relaxation modulus.

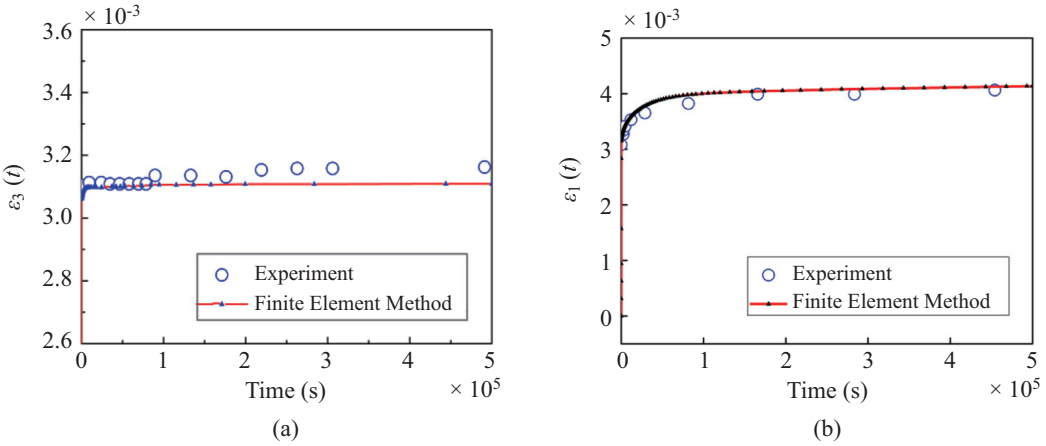


Fig. 5 Comparison of creep strain for unidirectional fiber reinforced composites, (a) force along the fiber direction (b) force along the fiber transverse direction.

https://doi.org/10.1017/jmech.2018.48 Published online by Cambridge University Press

$$
\begin{aligned}
&N_{i11}(t+\Delta t)\\
&=\int_{0^-}^{t+\Delta t} b_{i11} e^{-\frac{\int_{0^-}^{t+\Delta t}\frac{1}{a_T(T(\tau'))}d\tau'-\int_{0^-}^{\tau}\frac{1}{a_T(T(\tau'))}d\tau'}{\tau_1}}\dot{\varepsilon}_1 d\tau\\
&=N_{i11}(t)e^{-\frac{\int_{t}^{t+\Delta t}\frac{1}{a_T(T(\tau'))}d\tau'}{\tau_1}}\\
&+\int_{t}^{t+\Delta t} b_{i11} e^{-\frac{\int_{t}^{t+\Delta t}\frac{1}{a_T(T(\tau'))}d\tau'-\int_{0^-}^{\tau}\frac{1}{a_T(T(\tau'))}d\tau'}{\tau_1}}\dot{\varepsilon}_1 d\tau
\end{aligned}
\tag{20}
$$

As $\Delta t \to 0$, the equations above can be simplified as

$$
M_{i1}(t+\Delta t)=M_{i1}(t)+a_{i1}\Delta\varepsilon_1 \tag{21}
$$

$$
\begin{aligned}
&N_{i11}(t+\Delta t)\\
&=e^{-\frac{\Delta t}{a_T(T(t))\tau_1}}N_{i11}(t)+b_{i11}\frac{\Delta\varepsilon}{\Delta t}\int_t^{t+\Delta t} e^{-\frac{\int_{\tau}^{t+\Delta t}\frac{1}{a_T(T(\tau'))}d\tau'}{\tau_1}}d\tau\\
&=e^{-\frac{\Delta t}{a_T(T(t)\tau_1}}N_{i11}(t)+b_{i11}\frac{\Delta\varepsilon}{\Delta t}a_T(T(t))\tau_1\left(1-e^{-\frac{\Delta t}{a_T(T(t)\tau_1}}\right)
\end{aligned}
\tag{22}
$$

Here, only ΔM_{i1} and ΔN_{i11} are expressed in detail since all the other terms can be obtained by using the same approach. Therefore, the increment of stresses and the material Jacobian matrix, $\partial\Delta\sigma/\partial\Delta\varepsilon$, can be obtained.

4. NUMERICAL RESULTS AND DISCUSSIONS

4.1 Viscoelastic Properties of 2.5D Woven Composites

To study the influences of weaving densities on viscoelasticity of the composites, the relaxation moduli of 2.5D woven SMPCs with different weft and warp arranged densities subjected to strains along X, Y and Z directions at 80°C are calculated by the approach developed in the paper. Periodic boundary conditions are applied on the RUC to ensure compatibility of the boundary displacement and continuity of the stress.

Take 2.5D woven SMPCs with warp arranged density of 9 tows/cm and weft arranged density of 6 tows/cm, for example, the influence of strain applied is firstly discussed. In order to more intuitively reflect the effects of weaving densities on the viscoelastic properties of 2.5D woven SMPCs, the relaxation parameter R_I (I = X, Y or Z) is defined as follows:

$$
R_I=\frac{E_I(0)-E_I(\infty)}{E_I(0)} \tag{23}
$$

where $E_I(0)$ and $E_I(\infty)$ represent the initial and asymptotic moduli along direction I, respectively. Clearly, R_I directly reflects the magnitude of the viscoelastic effect of the woven composites in direction I. Larger R_I corresponds to a stronger viscoelastic effect, and vice versa.

It can be seen from Table 1 that the initial modulus in direction X gradually increases with the increase of strain due to the enhanced squeeze between yarns and more straightened warp yarns. However, in small strain state, the magnitude of strain applied has no significant effects on both initial and asymptotic moduli, and the relaxation parameter nearly unchanged. Thus 0.1% strain is applied on the RUC in three principle directions to investigate the influence of weaving densities on 2.5D woven SMPCs.

Table 1 Initial moduli, asymptotic moduli and relaxation parameters under different strains.

Strain (%)	0.1	0.5	1	2
$E_X(0)$ (GPa)	4.08	4.09	4.111	4.14
$E_X(\infty)$ (GPa)	0.668	0.670	0.670	0.670
R_X(%)	83.61	83.61	83.69	83.84

Figure 6 shows the effects of warp arranged density N_p on the relaxation moduli. It is clear that E_X, E_Y and E_Z all increase with the increase of N_p and the effects on the modulus along direction X is more apparent. The results are in agreement with the conclusion obtained by Song *et al*. [14] about the effects of weaving densities on elastic moduli of 2.5D woven composites. Influences of the weft arranged density on relaxation moduli are also investigated and the results are presented in Fig. 7. It is shown that the relaxation modulus along direction Y increases with the increase of the weft arranged density, while the relaxation modulus in direction X sharply decreases with the increase of N_t. With the same increment of weft arranged density, the increments of the relaxation modulus E_Y roughly remain unchanged since the weft yarns are major load-bearing part when the load is along direction Y. The decrease of the relaxation modulus E_X is mainly due to the increase of the dip angle which would greatly reduce the load-carrying capacity along the warp direction. The way E_Z changes with N_t is a bit more complicated. With the increase of N_t, there is a small increment for initial modulus $E_Z(0)$ but a much greater decrease for asymptotic modulus $E_Z(\infty)$, thus the weft arranged density N_t could greatly influences the viscoelasticity of 2.5D woven SMPCs in direction Z.

As illustrated in Figs. 6(b) and 7(b), the relaxation effect in direction Y is rather weak since weft yarns are almost straight. Thus only the relaxation effects in directions X and Z are further discussed here, as shown in Figs. 8 and 9. Figure 8 shows that R_X decreases with the increase of warp arranged density for the SMPCs with the same weft arranged density (N_t = 6). Figure 9 shows that R_X first increases until it reaches a maximum and then decreases for the SMPCs with the same warp arranged density (N_p = 9). It is clear that R_Z decreases with the increase of N_p and increases with the increase of N_t. Moreover, the weaving densities have greater influence on viscoelasticity of 2.5D woven SMPCs in thickness direction compared to the warp direction.

4.2 Shape Memory Behaviors of 2.5D Woven Composites

Since the relaxation effect is rather weak in the weft

https://doi.org/10.1017/jmech.2018.48 Published online by Cambridge University Press

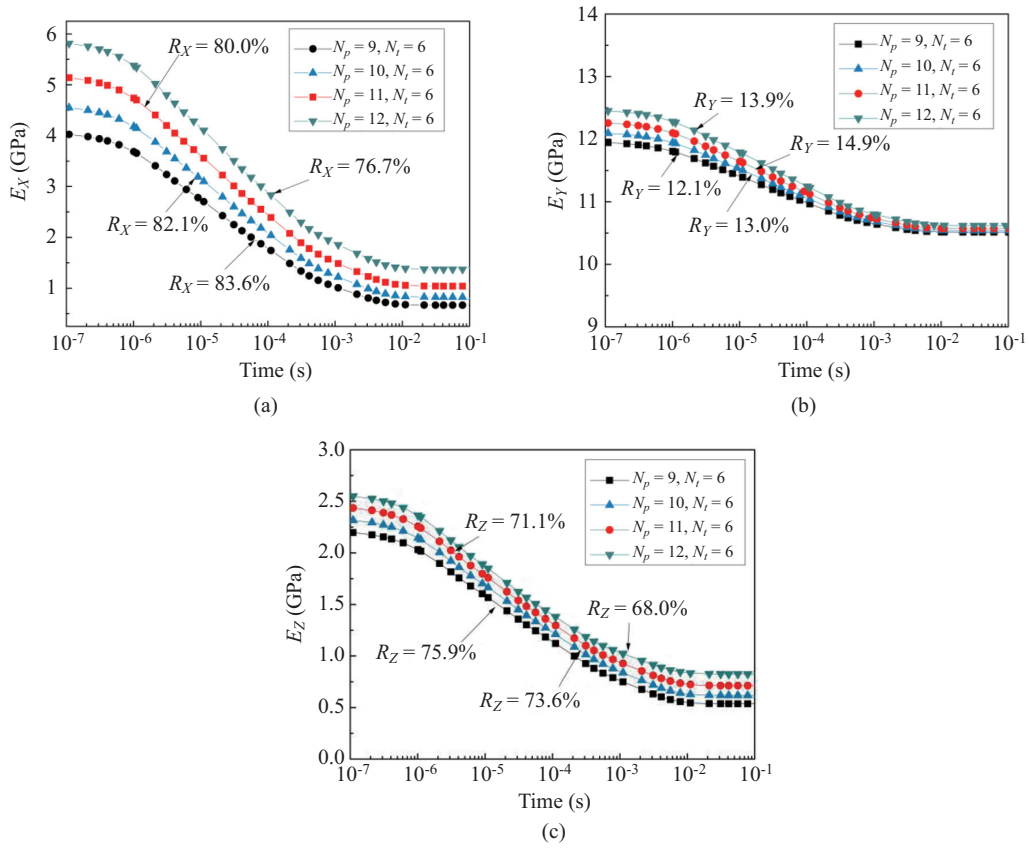


Fig. 6 Effects of warp arranged density on the relaxation moduli of 2.5D woven SMPCs at 80°C. (a) E_X (b) E_Y (c) E_Z

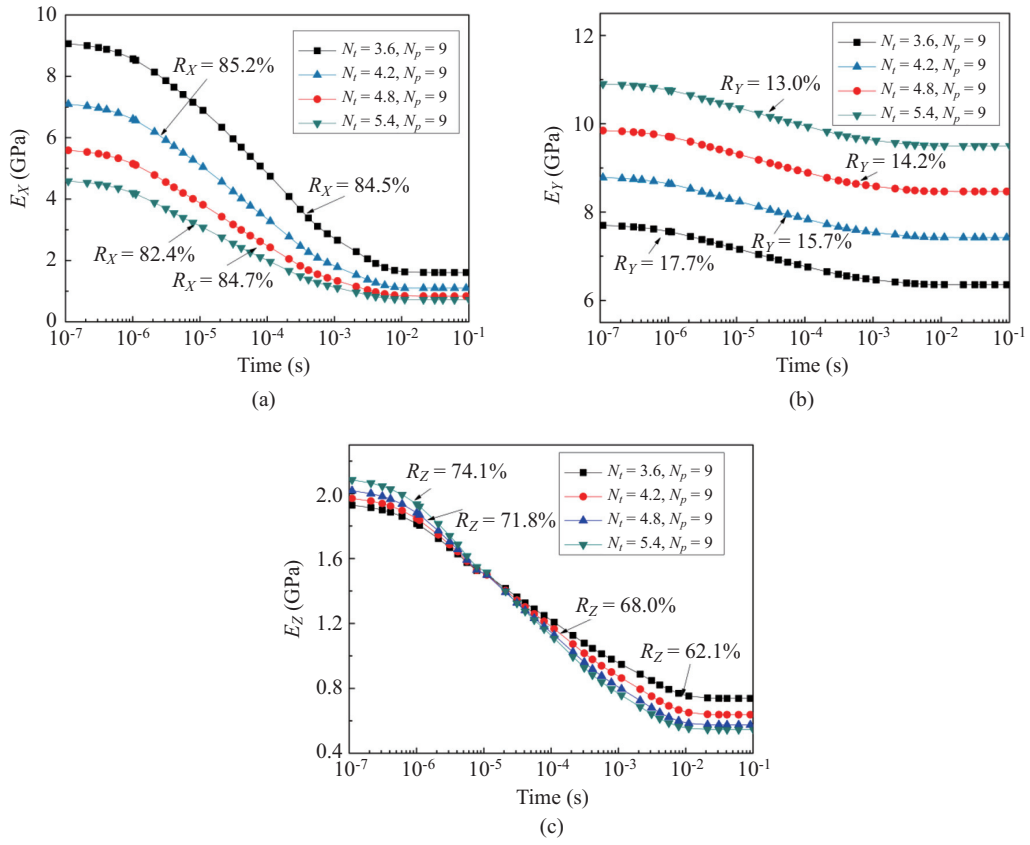


Fig. 7 Effects of weft arranged density on the relaxation moduli of 2.5D woven SMPCs at 80°C. (a) E_X (b) E_Y (c) E_Z.

https://doi.org/10.1017/jmech.2018.48 Published online by Cambridge University Press

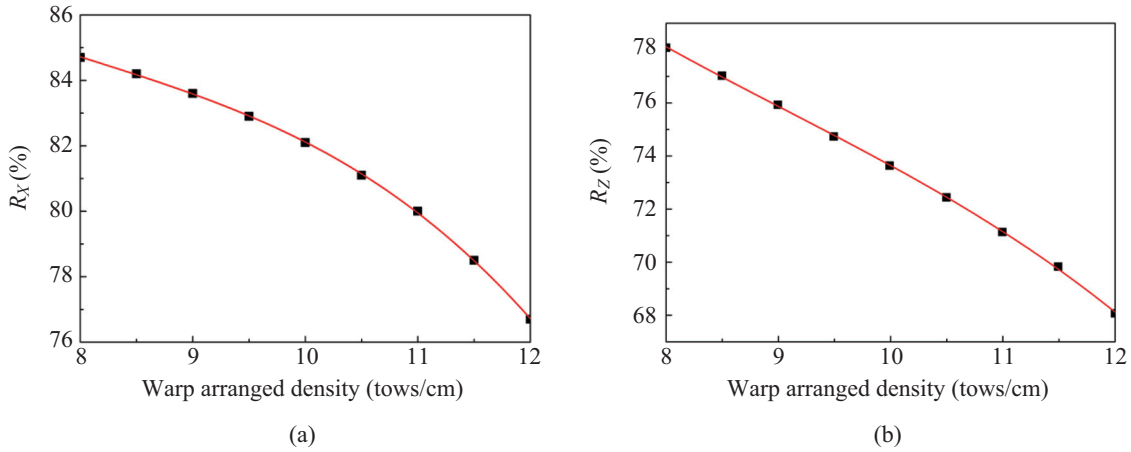


Fig. 8 Effects of warp arranged density on viscoelastic properties of 2.5D woven SMPCs.

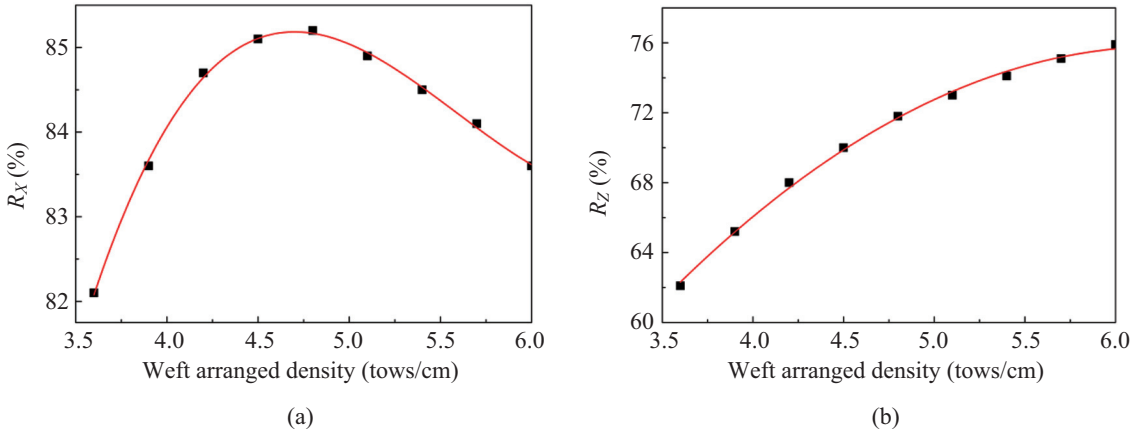


Fig. 9 Effects of weft arranged density on viscoelastic properties of 2.5D woven SMPCs.

direction, the in-plane shape memory effect of 2.5D woven composites discussed in the paper can only be realized in the warp direction. In the following, shape memory behaviors during the thermo-mechanical cycles with small tensile strain in direction X are studied in the paper. The thermo-mechanical cycle mainly consists of five steps. A pre-strain along direction X is gradually applied to the meso-RUC at the rate of 1%/min at 60°C (T_g + 23°C) in Step 1, and then the strain is fixed in Step 2 to finish the stress relaxation process. After that the material is cooled down to 30°C at a rate of -5°C/min in Step 3. The loading is removed in the following step, and part of the pre-deformed strain is retained. In the last step, the material is reheated to the initial temperature at 5°C/min, either in the condition of free-length recovery or length-constrained recovery. The strain recovery process could be measured in the free-length recovery while the stress recovery could be recorded in the length-constrained recovery. A 3D temperature-strain-stress graph reflecting the two kinds of recovery procedures for 2.5D woven SMPCs (N_p = 9, N_t = 6) is shown in Fig. 10.

The shape fixation ratio R_f can be defined as:

$$R_f = \frac{\varepsilon_{fix}}{\varepsilon_{pre}} \times 100\% \tag{24}$$

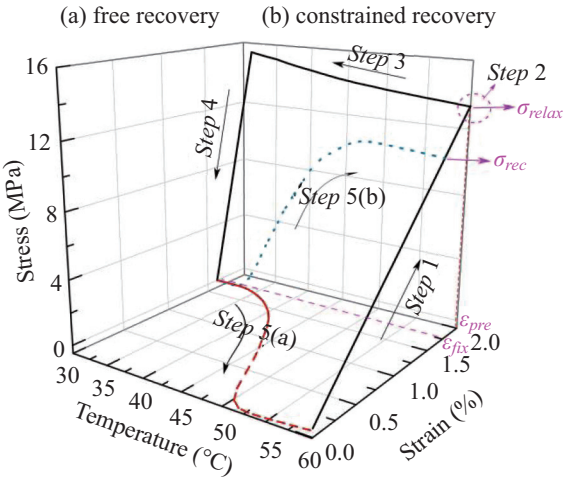


Fig. 10 Temperature-strain-stress graph reflecting two typical kinds of thermo-mechanical cycles of 2.5D SMPCs ((a) free-length recovery, (b) length-constrained recovery).

where ε_{pre} is the pre-deformed strain applied in Step 1 and ε_{fix} represents the retained strain at the end of Step 4 when the external force is removed, as illustrated in Fig. 10.

https://doi.org/10.1017/jmech.2018.48 Published online by Cambridge University Press

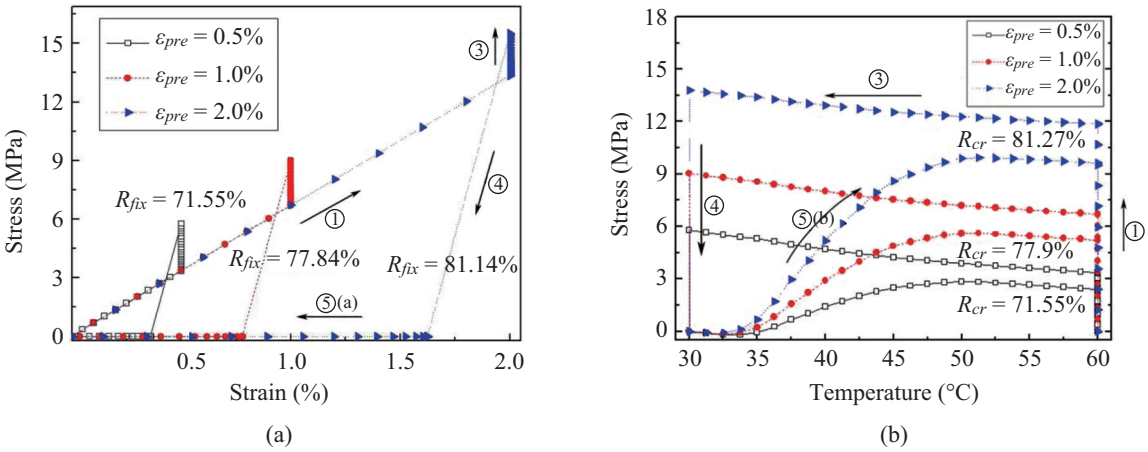


Fig. 11 Effects of pre-deformed strain on shape memory performance of 2.5D woven SMPCs. (a) Strain-stress graph in free-length recovery process, (b) Temperature-stress graph in length-constrained recovery process.

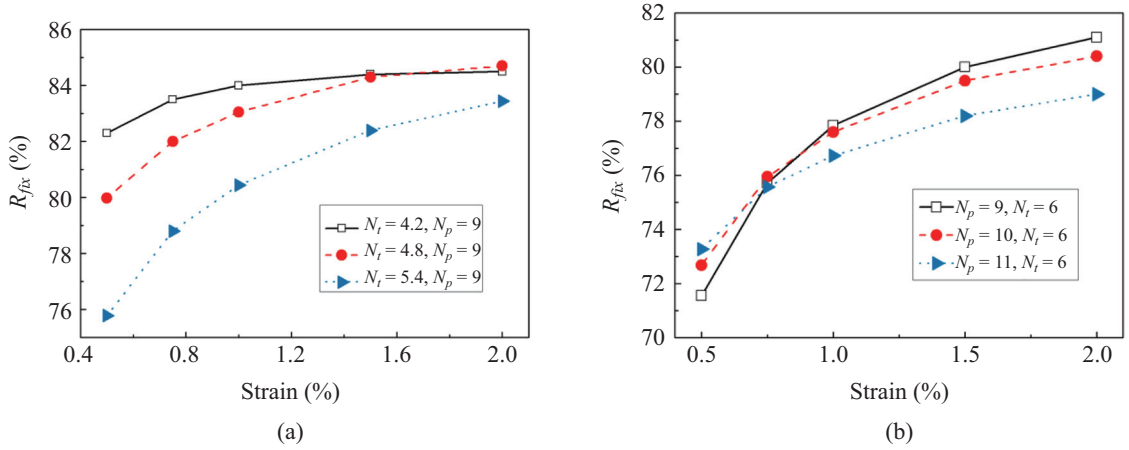


Fig. 12 Shape fixation ratios versus pre-deformed strains.

Similarly, stress recovery ratio R_{rec} is defined as:

$$R_{cr} = \frac{\sigma_{rec}}{\sigma_{relax}} \times 100\% \tag{25}$$

where σ_{relax} is the equivalent stress after stress relaxation in Step 2 and σ_{rec} is the stress at the end of Step 5 when the material is reheated to initial temperature with retained strain constrained.

As illustrated in Fig. 10, the stress linearly increases with the strain when the SMPC is stretched at a high temperature in Step 1. Stress relaxation is not obvious in Step 2 due to the low strain loading rate in the previous step. During the stress-freezing process, the equivalent stress shows a gradually increase with the decrease of temperature. When the temperature is lower than T_g, the increasing rate of the equivalent stress remarkably increases since the relaxation rate of stress caused by thermal strain slows down rapidly. After removal of the external force, part of the pre-deformed strain springs back. In the free-length recovery process, the frozen strain is gradually released, and the shape recovery rate accelerates near T_g. The shape completely recover to the initial state when the temperature is raised to 60°C, and the shape recovery ratio is nearly 100%. During the length-constrained recovery process, the recovery stress at the end of Step 5 is close to 10 MPa, which is significantly higher than that of pure SMP (0.13 MPa). It is favorable for its use as a driving device in the space deployable structures.

The effect of pre-deformed strain on shape memory performance is also investigated. Pre-deformed strain varying from 0.5% to 2.0% is applied to 2.5D woven SMPCs with warp arranged density of 9 tows/cm and weft arranged density of 6tows/cm. Both free-length recovery and length-constrained recovery procedures are recorded. The results are shown in Fig. 11.

As shown in Fig. 11(a), shape fixation ratios increase with the increase of pre-deformed strain, which indicates that thermal strain has a significant effect on shape fixation ratios of 2.5D woven SMPCs when small strain is applied on the SMPC. In the case of small strain, the deformed shape could always recover to the initial state with a shape recovery ratio of nearly 100% after heating to the high temperature since there is no fiber damage. Therefore, the shape recovery ratio is no longer the focus

https://doi.org/10.1017/jmech.2018.48 Published online by Cambridge University Press

in the following discussion. It can also be seen from Fig. 11(b) that stress recovery ratios increase with the increase of pre-deformed strain, and the results show that it is basically consistent with the shape fixation ratio.

The influence of weaving densities on shape memory performance of 2.5D woven SMPCs is further discussed. Figure 12 is the summary of shape fixation ratios versus pre-deformed tensile strains with variations of warp or weft arranged densities. As shown in the figure, the influence of pre-deformed strain on shape fixation ratio decreases with the increase of warp arranged density and increases with the increase of weft arranged density. It can be found that, with the increase of pre-deformed strain, the proportion of thermal strain decreases, and the fixation ratio R_{fix} gradually approaches the relaxation parameter R_X. Therefore, it could be concluded that the influence of weaving densities on shape fixation ratio should be consistent with that on the viscoelastic properties along the warp direction. Furthermore, it can also be deduced that when a relatively large pre-deformed strain or a bending deformation is applied on the SMPCs in the warp direction, the shape fixation ratio could be predicted with the relaxation parameter since the effect of thermal strain is negligible.

5. CONCLUSIONS

Thermo-mechanical properties of 2.5D woven angle-interlock SMPCs are investigated in the paper with a multi-scale strategy. In the multi-scale modeling approach, mesoscopic model of 2.5D woven SMPCs and microscopic model of yarns are developed, respectively. Thereafter, the constitutive model and the programming method of FEM for the yarns are presented. In the work, the effect of weft and warp arranged densities on the viscoelastic properties is firstly studied based on the modeling approach. Furthermore, two typical kinds of thermo-mechanical cycles are simulated to investigate the shape memory behaviors of 2.5D woven SMPCs. It is found that the influence of weaving densities on shape fixation ratio should be consistent with that on the viscoelastic properties along the warp direction. The study in the paper proposes a feasible approach for further investigation of 2.5 woven SMPCs, and lays a foundation for their design and application in engineering.

ACKNOWLEDGEMENTS

The research is supported by the National Natural Science Foundation of China (Grant Nos. 11572153, 11272104), the Natural Science Foundation of Jiangsu Province of China (BK20170759, BK20151467), a project funded by the Priority Academic Program Development of Jiangsu Higher Education Institutions (PAPD), Outstanding Scientific and Technological Innovation Team in Colleges and Universities of Jiangsu Province and the Doctor Special Foundation and the Research Fund of Nanjing Institute of Technology (ZKJ201603).

REFERENCES

1. Leng, J. S., Lan, X., Liu, Y. J. and Du, S. Y., "Shape-Memory Polymers and Their Composites: Stimulus Methods and Applications," *Progress in Materials Science*, **56**, pp. 1077-1135 (2011).
2. Leng, J. S., Lu, H. B., Liu, Y. J., Huang, W. M. and Du, S. Y., "Shape-Memory Polymers—A Class of Novel Smart Materials," *Mrs Bulletin*, **34**, pp. 848-855 (2009).
3. Hu, J., Zhu, Y., Huang, H. and Lu, J., "Recent Advances in Shape-Memory Polymers: Structure, Mechanism, Functionality, Modeling and Applications," *Progress in Polymer Science*, 37, pp. 1720-1763 (2012).
4. Hager, M. D., Bode, S., Weber, C. and Schubert, U. S., "Shape Memory Polymers: Past, Present and Future Developments," *Progress in Polymer Science*, **49**, pp. 3-33 (2015).
5. Zhao, Q., Qi, H. J. and Xie, T., "Recent Progress in Shape Memory Polymer: New Behavior, Enabling Materials, and Mechanistic Understanding," *Progress in Polymer Science*, **49**, pp. 79-120 (2015).
6. Zhang, C. S. and Ni, Q. Q., "Bending Behavior of Shape Memory Polymer Based Laminates," *Composite Structures*, **78**, pp. 153-161 (2007).
7. Ahmad, M., Singh, D., Fu, Y. Q., Miraftab, M. and Luo, J. K., "Stability and Deterioration of A Shape Memory Polymer Fabric Composite under Thermo-mechanical Stress," *Polymer Degradation and Stability*, **96**, pp. 1470-1477 (2011).
8. Roh, J. H., Kim, H. J. and Bae, J. S., "Shape Memory Polymer Composites with Woven Fabric Reinforcement for Self-deployable Booms," *Journal of Intelligent Material Systems and Structures*, **25**, pp. 2256-2266 (2014).
9. Nji, J. and Li, G. Q., "A Self-Healing 3D Woven Fabric Reinforced Shape Memory Polymer Composite for Impact Mitigation," *Smart Materials and Structures*, **19**, pp. 35007-35015 (2010).
10. Tan, P., Tong, L. and Steven, G. P., "A Three-Dimensional Modeling Technique for Predicting the Linear Elastic Property of Opened-Packing Woven Fabric Unit Cells," *Composite Structures*, **38**, pp. 261-271 (1997).
11. Tan, P., Tong, L. and Steven, G. P., "Applied Science And Manufacturing : Micromechanics Models For Mechanical And Thermomechanical Properties Of 3D Through-The-Thickness Angle Interlock Woven Composite," *Composites Part A-Applied Science and Manufacturing*, **30**, pp. 637-648 (1999).
12. Hallal, A., Younes, R., Fardoun, F. and Nehme, S., "Improved Analytical Model to Predict the Effective Elastic Properties of 2.5D Interlock Woven Fabrics Composite," *Composite Structures*, **94**, pp. 3009-3028 (2012).
13. Lu, Z. X., Zhou, Y., Yang, Z. Y. and Liu, Q., "Multi-

https://doi.org/10.1017/jmech.2018.48 Published online by Cambridge University Press

Scale Finite Element Analysis of 2.5D Woven Fabric Composites under On-axis and Off-axis Tension," *Computational Materials Science*, **79**, pp. 485-494 (2013).

14. Song, J., Wen, W., Cui, H., Zhang, H. and Xu, Y., "Finite Element Analysis of 2.5D Woven Composites, Part I: Microstructure and 3D Finite Element Model," *Applied Composite Materials*, **23**, pp. 29-44 (2016).
15. Song, J., Wen, W., Cui, H., Zhang, H. and Xu, Y., "Finite Element Analysis of 2.5D Woven Composites, Part II: Damage Behavior Simulation and Strength Prediction," *Applied Composite Materials*, **23**, pp. 45-69 (2016).
16. Liu, Y., Gall, K., Dunn, M. L., Greenberg, A. R. and Diani, J., "Thermomechanics of Shape Memory Polymers: Uniaxial Experiments and Constitutive Modeling," *International Journal of Plasticity*, **22**, pp. 279-313 (2006).
17. Tobushi, H., Hashimoto, T., Hayashi, S. and Yamada, E., "Thermomechanical Constitutive Modeling in Shape Memory Polymer of Polyurethane Series," *Journal of Intelligent Material Systems and Structures*, **8**, pp. 711-718 (1997).
18. Tobushi, H., Okumura, K., Hayashi, S. and Ito, N., "Thermomechanical Constitutive Model of Shape Memory Polymer," *Mechanics of Materials*, **33**, pp. 545-554 (2001).
19. Diani, J., Liu, Y. and Gall, K., "Finite Strain 3D Thermoviscoelastic Constitutive Model for Shape Memory Polymers," *Polymer Engineering and Science*, **46**, pp. 486-492 (2006).
20. Nguyen, T. D., Qi, H. J., Castro, F. and Long, K. N., "A Thermoviscoelastic Model for Amorphous Shape Memory Polymers: Incorporating Structural and Stress Relaxation," *Journal of the Mechanics and Physics of Solids*, **56**, pp. 2792-2814 (2008).
21. Diani, J., Gilormini, P., Frédy, C. and Rousseau, I., "Predicting Thermal Shape Memory of Crosslinked Polymer Networks from Linear Viscoelasticity," *International Journal of Solids and Structures*, **49**, pp. 793-799 (2012).
22. Tian, J. and Zhou, C. W., "Multi-Scale Coupled Numerical Analysis of Textile Composites and Structures," *Chinese Journal of Computational Mechanics*, **27**, pp. 1022-1028 (2010).
23. Arrieta, S., Diani, J. and Gilormini, P., "Experimental Characterization and Thermoviscoelastic Modeling of Strain and Stress Recoveries of An Amorphous Polymer Network," *Mechanics of Materials*, **68**, pp. 95-103 (2014).
24. Schapery, R., "Thermal Expansion Coefficients of Composite Materials Based on Energy Principles," *Journal of Composite Materials*, **2**, pp. 380-404 (1968).
25. Megnis, M. and Varna, J., "Micromechanics Based Modeling of Nonlinear Viscoplastic Response of Unidirectional Composite," *Composites Science and Technology*, **63**, pp. 19-31 (2003).

(Manuscript received January 25, 2018,
accepted for publication August 7, 2018.)

https://doi.org/10.1017/jmech.2018.48 Published online by Cambridge University Press